Experimental

Materials

Locust Bean Gum, K-carrageenan and Xanthan Gum were generous gift samples from Cargill R&D (Vilvoorde, Belgium). Sunflower oil and monoglycerides (distilled monoglycerides from sunflower oil) were received as gift samples from Vandemoortele R&D Izegem, Belgium. Rhodamine B was purchased from Sigma Aldrich Inc. (USA). Distilled water was used for all the experiments.

Locust Bean Gum

Carrageenan

Xanthan gum

Fig. 6. Molecular structures of hydrocolloids used in emulsion preparation.

Preparation of HIPE gels

For initial trials, HIPE were prepared using monoglycerides and PGPR as emulsifiers. Both water and oil phases (containing emulsifier) were heated >70°C followed by shearing at 11,000 rpm with the help of a high energy dispersing unit (Ultraturrax® (IKA®-Werke GmbH & Co. KG, Germany). The sheared liquid mixtures were then cooled to room temperature to get emulsions. For HIPE gels, hydrocolloid dispersions were used as water phases and the above procedure was repeated. Emulsion gels were prepared using different hydrocolloid combinations and varying the total polymer concentrations as well as hydrocolloid proportions as tabulated below (for emulsions with $\varphi_{water} = 0.75$). The emulsions prepared using hydrocolloids showed immediate gelling when the shearing was stopped. Emulsion & emulsion gels were stored at 5 °C until used for further experiments.

Table 1: Ingredients used for preparing emulsions ($\varphi_{water} = 0.75$) using 0.4 %wt of PGPR as emulsifier and a varying total polymer concentrations (LBG and CAR or LAB and XAN) at different proportions.

Ingredients	% wt	Samples					
	% wt	%wt	%wt	%wt	%wt	%wt	%wt
Water	77.00	77.00	77.00	77.00	77.00	77.00	77.00
Oil	21.85	21.60	21.35	21.10	21.60	21.60	21.60
PGPR	0.40	0.40	0.40	0.40	0.40	0.40	0.40
LBG	0.57	0.75	0.94	1.12	0.50	0.25	0.75
CAR	0.18	0.25	0.31	0.38	0.50	0.75	-
XAN	-	-	-	-	-	-	0.25
Total	100	100	100	100	100	100	100

From a practical point of view, it is important to note that the shearing of emulsion has to be carried out at high temperature (>70°C) to ensure homogenous mixing of two phases. The gelation of emulsions occurs very rapidly after shearing so the post handling of the emulsion gels (filling in cups of desired sizes for texture measurements) should be well planned.

Characterization of HIPE gels

Microstructure studies

The microstructure of emulsions and emulsion gels was studied using optical light microcopy (Leica DM2500 microscope, Leica Microsystems, Belgium). For confocal microscopy, Rhodamine B was dissolved in water phase prior to preparing the emulsion gel. Samples were imaged using a Nikon A1R confocal microscope (Nikon Instruments Inc., USA). Excitation was performed by means of a 488nm Ar laser and fluorescence was detected through a 525/50 bandpass filter. Images were acquired and processed with Nikon NIS Elements software. For cryo-SEM, samples of emulsion gel were placed in the slots of a stub, plunge-frozen in liquid nitrogen and transferred into the cryo-preparation chamber (PP3010T Cryo-SEM Preparation System, Quorum Technologies, UK) where it was freeze-fractured and subsequently sputter-coated with Pt and examined in JEOL JSM 7100F SEM (JEOL Ltd, Tokyo, Japan).

Droplet size analysis

Water droplet size analysis of the w/o emulsions and emulsion gels was performed by pulsed field gradient Nuclear Magnetic Resonance (pfg-NMR) on a benchtop Maran Ultra spectrometer (Oxford Instruments, UK) operating at a frequency of 23.4 MHz in combination with the Droplet size application (Resonance Instruments Ltd.). Samples were analysed at 5 °C to minimize inter-droplet water diffusion. To suppress the NMR contribution of the fat phase, pfg-NMR experiments were conducted using an inversion recovery-stimulated echo pulse sequence. In the performed experiments, the diffusion time (Δ) was set to 0.2 seconds, the gradient strength was fixed at 1.74 T/m, while the gradient duration (δ) was varied in 17 steps from 400 to 4500 ms. By measuring the echo attenuation ratio of the NMR signal as a function of the gradient duration, it is possible to determine the hindered diffusion behaviour and hence the droplet size distribution.

Texture analysis

The emulsion gels were subjected to penetration and compression (relaxation and texture profile analysis (TPA) on a texture analyser (Instron Model 5942, USA). For penetration tests, 20 g samples were placed in 50 ml plastic containers and a probe with a cylindrical probe (diameter of 12 mm) was penetrated to 15mm at a constant speed of 50mm/min. Factors like critical force and the fracture strain (compressive extension) at the yield point was obtained from the load-displacement curves and the modulus of elasticity (E_y) was calculated using the following formula:

$$E_y = \sigma / \gamma = F.l / A.\Delta l = k.l / A$$

Where, E_y: modulus of elasticity (N/m^2)
$\quad\quad$ F: force applied on the sample (N)
$\quad\quad$ $l*$: displacement of the sample until the breaking point (m)
$\quad\quad$ A: cross-sectional area through which the force is applied (probe) (m^2)
$\quad\quad$ $k = F/\Delta l$: slope of the straight line portion of the load-displacement curve (N/m)

For relaxation test, gels were first set into cylindrical samples of 8 mm height and 1 mm diameter. A cylindrical probe (diameter 40mm) was used to compress the samples to a strain of 37.5 % (well below the fracture strain) followed by holding at this strain for 200s. The stress relaxation curves were plotted by recording the stress as a function of time while the strain was kept constant (**Fig. 6**).
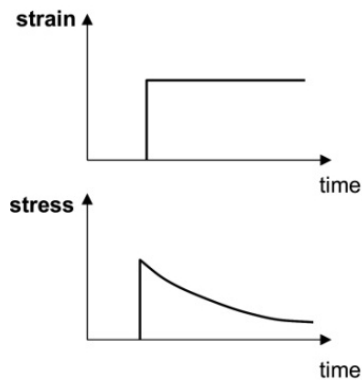
Fig. 7. Graphical representation of stress relaxation test where an instantaneous strain is kept constant and simultaneously stress is recorded as a function of time.

For TPA analysis, cylindrical samples of (8 mm height and 1 mm diameter) were subjected to a 2 step compression test using a cylindrical probe (40 mm diameter) at a speed of 10mm/min. The first cycle comprised of compressing the sample to 50 % of its height (50 % strain) followed by removal of load through upward movement of the probe. The whole cycle was repeated in step 2. The measured force during these 2 cycles as a function of time was plotted to get a TPA curve (**Fig. 7**). Measurements were done on 10 replicates of each samples.
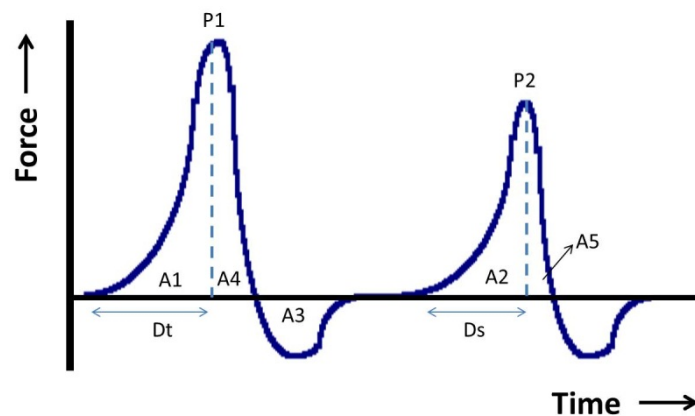
Fig. 8. Typical TPA curve which indicators (A = area, P = point and D = distance) which can be used for calculation of textural parameters such as:

Firmness (Hardness) 1: P1; Firmness (Hardness) 2: P2; Cohesiveness: A2/A1; Adhesiveness: A3; Springiness: Ds/Dt; Resilience: A4/A1; Chewiness: Hardness x Cohesiveness
Fracturability (Not shown): Fracturability point occurs where the plot has its first significant peak during the first compression cycle.

Statistical analysis

Data from texture profile analysis were compared using statistical analysis. An unpaired, two-tailed student T-test was used on the data to establish statistical significance in the differences observed.
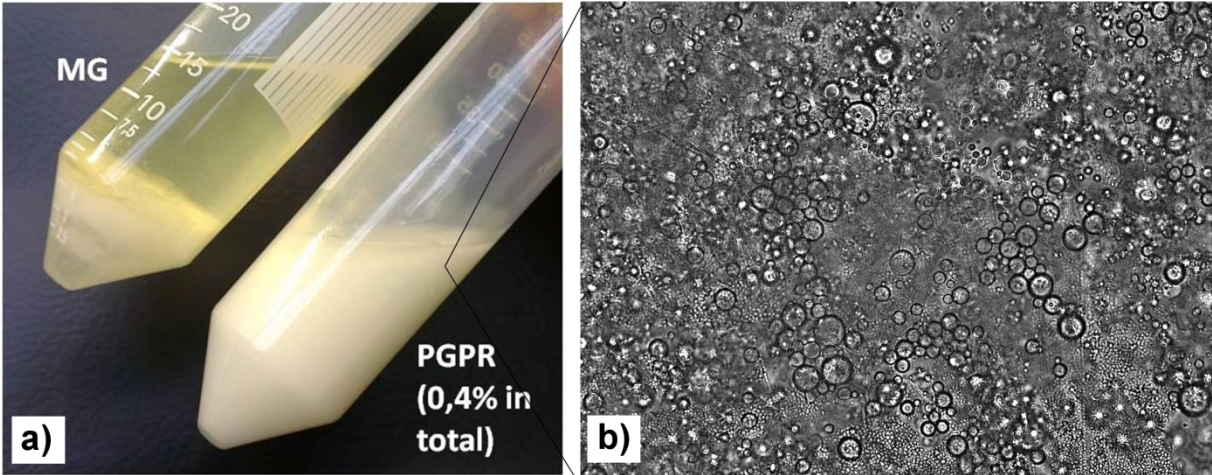
Figures

Fig S1: a) Photograph of w/o emulsions prepared at ϕ_{water} = 0.75 using monoglycerides (MG) and Polyglycerol polyricinoleate (PGPR). Notice how MG was unable to form a stable emulsion even at 5 %wt concentration compared to PGPR that gave a stable emulsion at a relatively low concentration of 0.4 %wt; b) Optical microscopy image of HIPE emulsions prepared using PGPR as an emulsifier.
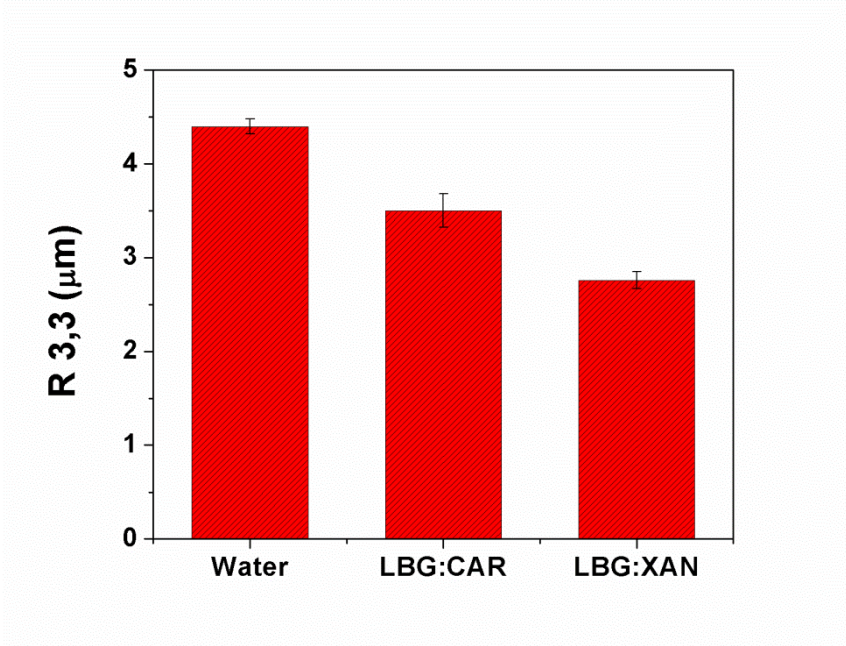

Fig S2: Volume weighted droplet radius (R3,3) of emulsions prepared at ϕ_{water} = 0.75 without and with hydrocolloids in the water phase.
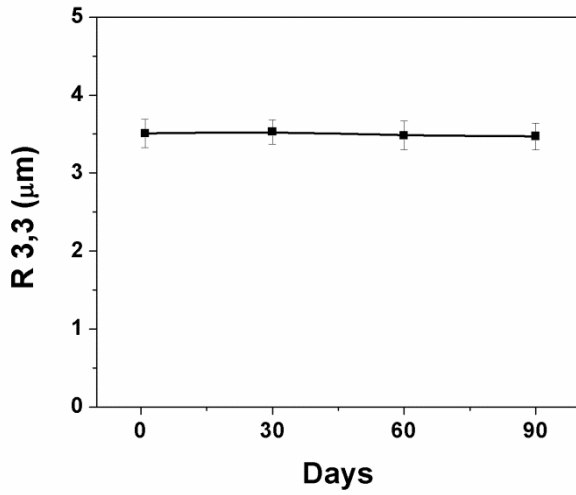
Fig S3: Volume weighted droplet radius (R3,3) of HIPE gel prepared at ϕ_{water} = 0.75 using LBG:CAR (75:25) over 3 months of storage.

Table 1: Fracture properties of HIPE gels evaluated using uni-axial compression tests.

Fracture properties	Polymer concentration			
	0.75 %wt	**1.0 %wt**	**1.25 %wt**	**1.5 %wt**
Critical Force (N)	0.69 ± 0.03	1.39 ± 0.01	2.17 ± 0.01	3.07 ± 0.04
Young's Modulus (Nm^{-2})	4.62 ± 0.01	9.33 ± 0.03	15.78 ± 0.04	23.23 ± 0.03
Displacement at fracture point (mm)	14.86 ± 0.001	13.42 ± 0.003	10.67 ± 0.005	9.92 ± 0.003

Fracture properties	LBG:CAR ratios		
	25:75	**50:50**	**75:25**
Critical Force (N)	1.25 ± 0.02	2.65 ± 0.03	1.39 ± 0.01
Young's Modulus (Nm^{-2})	9.57 ± 0.13	19.18 ± 0.32	9.33 ± 0.11
Displacement at fracture point (mm)	3.59 ± 0.002	6.75 ± 0.004	13.42 ± 0.003